Pacific Warm Pool Temperature Regulation during TOGA COARE: Upper Ocean Feedback

Gary S.E. Lagerloef
Earth and Space Research, 1910 Fairview Ave. E., Suite 102, Seattle, WA 98102

Roger Lukas
Department of Oceanography, University of Hawaii, 1000 Pope Rd., Honolulu, HI 96822

Robert A. Weller and Steven P. Anderson
Department of Physical Oceanography, Woods Hole Oceanographic Institution, Woods Hole, MA 02543

For submission to Journal of Climate (accepted),

Revised: 2 December 1997

Abstract

The Hasselmann feedback model was applied to hindcast western Pacific warm pool sea surface temperatures (SST) with heat flux observations obtained near 2°S 156°E from October 1992 - February 1993 during TOGA COARE . The model versus observed SST correlations were greater than 0.85. Two important feedback (or damping) time scales emerged, with e−folding times of λ^{-1}=0.2 days and 8 days, fitting to the diurnal and sub-diurnal variations respectively. Distinct mixed layer depth scales were also found for the respective time scales. A time varying depth parameter with a median of ~5 m was derived for the shorter time scale, and varied with the observed daily minimum mixed layer depth. A constant ~16 m was optimal for the longer time scale, which is similar to the time-averaged observed mixed layer depth of 14.8 m and the Monin-Obukhov scale of ~17 m. This bears on the choice of mixed layer parameters for climate model simulations of warm pool conditions observed in TOGA COARE. The low frequency time and depth scale parameters give a negative feedback of about 95 Wm^{-2} $^{o}C^{-1}$, which is significantly greater than previous studies have indicated. This restoring influence was treated separately from fluxes across the air-sea interface such as latent, radiative and sensible heat loss or cloud shading, and is thus attributed to oceanic mixed layer processes. The frequency band where the damping or feedback becomes important is defined by $\omega \approx \lambda$, which we find coincides with the diurnal cycle and the ~50 d Madden-Julian oscillations (MJO) for the respective λ^{-1} time scales. This indicates a possible dynamic connection between the surface heat forcing and mixed layer dissipation time scales, which we suggest might be accounted for if the dissipation is parameterized as being proportional to the amplitude of SST variations.

1. Introduction

Hasselmann (1976) proposed a stochastic climate model whereby low frequency fluctuations are treated as an accumulation of forcing events with a damping or feedback term. The

simplest 1−D formulation is:

$$\frac{\partial T}{\partial t} = F - \lambda T \tag{1}$$

where T is any climate variable anomaly, F is the forcing variable, λ is the damping coefficient with units of t^{-1} and t is time. This formula is equivalent to a linear first order mechanical system (Jenkins and Watts, 1968, ch. 2.3), and the output is a first order Markov process when F is random white noise. Frankignoul (1985) gives a thorough treatment with regard to SST anomalies and feedbacks in the mid latitudes. In general, a stochastic approach is taken whereby the atmospheric forcing is assumed to be white noise and the ocean response has a spectrum proportional to $(\omega^2 + \lambda^2)^{-1}$, where $\omega=2\pi f$ and f is frequency. This spectrum appears evident in SST observations (Frankignoul and Hasselmann 1977) and within certain mid-latitude regions in recent coupled model simulations (Manabe and Stouffer, 1996). Frankignoul and Reynolds (1983) estimated λ by fitting observed SST spectra and obtained decay times (λ^{-1}) of 2 to 6 months in the North Pacific, and they also showed that the lagged correlations between EOFs of SST and flux terms were consistent with the model. The spectral fitting approach requires time series which are much longer than the decay time scale so that frequencies $<<\lambda$ are resolved. Alternatively, with measurements of both the forcing and response, Eq. (1) can be integrated forward with various λ to find a value that produces the best fit between the model and observed response. Lagerloef (1995) took this approach to study interdecadal dynamic height variations in the Alaska Gyre when F was attributed to Ekman pumping.

The same approach is used here to examine a ~4 month record of net heat flux and SST obtained western equatorial Pacific warm pool region during TOGA COARE (see Webster and Lukas, 1992 for a complete description of the field measurement program.). Heat flux measurements with an uncertainty of <10 Wm^{-2} have been obtained (Weller and Anderson, 1996). Such precise measurements allow Eq. (1) to be tested quantitatively in the warm pool region. The model is applied in a deterministic manner (rather than stochastically) to predict

the response, T, to measured fluxes and compare with the observed SST. A positive result from such a simple feedback parameterization will force us to consider the implications of the numerical value of λ on the physical process which regulate SST in the warm pool region.

2. Measurements:

The extensive measurements made of the upper ocean and troposphere during COARE included air/sea fluxes and SST from several surface platforms. Most of the attention was focused on an Intensive Flux Array (IFA) and a cluster of observations centered near 2°S and 156°E in the heart of the warm pool. The specially-engineered Improved Meteorological (IMET) mooring (Weller and Anderson, 1996) was one of the primary observing systems, and measured shortwave and longwave fluxes, near surface ocean temperature, and variables used to derive latent and sensible heat fluxes. The sensors are described by Hosum, et al, (1995). The buoy was situated at 1.75°S and 156°E during the COARE Intensive Observing Period (IOP) from 21 October 1992 to 3 March 1993. The data are continuous except for a 4-day gap beginning 9 December, which was patched with duplicate observations from a nearby platform or by duplicating the prior 4 day record, and other small gaps which were interpolated. The shallowest IMET temperature measurement was at 0.45 m, which we use as an index of both the mixed layer temperature and of SST. It remains an approximation, although often used, to equate the actual surface temperature with the near surface mixed layer temperature. It should be noted that episodes of strong temperature gradients within the upper 0.5 m were observed during the COARE IOP (e.g., Soloviev and Lukas, 1996).

The net surface heat flux into the ocean is given by $Q_{net}=Q_{sw}-Q_{lw}-Q_{lat}-Q_{sen}$, where Q_{sw} is the shortwave radiation (positive downward) and Q_{lw}, Q_{lat}, Q_{sen} are the longwave radiation, latent and sensible fluxes (positive upward) derived from IMET sensors using the COARE flux algorithm (Fairall, et al, 1996). The Q_{net} signal is dominated by the strong daytime insolation heating and night-time cooling cycle, with some lower frequency modulations (top panel of Fig 1). SST episodically exhibits a strong diurnal cycle superimposed on much lower

frequency variations, as shown by the light curve in the second panel of Fig. 1. These low frequency variations are much more prominent in the SST signal than Q_{net}, and such frequency separation is characteristic of the feedback model (see Sect. 5, below).

3. Intraseasonal Variations and Modeling

A simplified one-dimensional mixed layer heat budget is expressed as:

$$\frac{\partial T}{\partial t} = \frac{Q_{net} - rQ_{sw}}{h\rho C_p} + M \qquad (2)$$

where T is mixed layer temperature, h is the surface mixed layer depth scale, ρ and C_p are the density and specific heat of seawater respectively and M is the aggregate of upper ocean processes providing heat dissipation from the mixed layer. The coefficient r is the fraction of Q_{sw} which penetrates the surface layer of depth h to the waters below. Siegel, et al. (1995), their Fig. 2, report a nominal value of $r \approx 0.2$ for $h \approx 15$ m in the IFA during COARE, ranging from about 0.1 to 0.3 depending on the biomass concentration. In this analysis we make the simplifying assumption r=0, and show in the Appendix that this does not affect the salient features of the feedback modeling results. In relating Eqs. (1) and (2), we see that F corresponds to the net surface fluxes in the first term on the right hand side of (2), and that λT parameterizes the collective effects of M. We note that Q_{net} contains terms which are dependant on SST, but these feedbacks are not accounted for in λT. Rather, they remain included in the observed fluxes used to force the model. By inference, λT parameterizes only mixed layer processes that do not involve flux across the air-sea interface. A null result of $\lambda \neq 0$ implies that such non air-sea fluxes are important, whereas $\lambda = 0$ implies air-sea feedback dominates. This is a slight departure from the development given by Frankignoul (1985) where air-sea flux and oceanic terms could appear in both the forcing and feedback. The intention here is not to fully diagnose the various dissipation or feedback mechanisms, but rather to learn what we can from testing this simple parameterization. We therefore apply the

model to COARE data using:

$$\frac{\partial T}{\partial t} = \frac{Q_{net}}{h\rho C_p} - \lambda T \tag{3}$$

In finite difference form, this is expressed as a first order autoregression process:

$$T_{i+1} = \frac{Q_i}{h\rho C_p} dt + (1 - \lambda dt)T_i \tag{4}$$

where $dt=t_{i+1} - t_i$ and Q_i represents Q_{net} at time t_i. Henceforth, the notation T will signify a result derived from (4), while SST will signify the observed temperature at 0.45 m depth.

It will become apparent below that it was convenient to separate the diurnal from the low frequency variations. A Butterworth low pass filter (half power at 0.48 cpd) was applied, designated henceforth as SST_{lo} and Q_{lo}. High pass data then were obtained by $SST_{hi}=SST-SST_{lo}$ and $Q_{hi}=Q-Q_{lo}$ respectively.

The spectral nature of T is governed by λ, whereas a constant coefficient h determines the amplitude of T relative to $Q_{net}/\rho C_p$. The layer thickness scale h determines an effective heat capacity for the thermodynamically active mixed layer. T is modeled as an anomaly from an equilibrium value and evolves according to (4), becoming independent of the initial value at times $t>1/\lambda$. We wish to determine the values of the parameters, λ and h, which provide the best fit between T and SST. This was done through a combination of trial and error and linear regression. We initially set $h=h_c=1$ m, since any constant h will yield the same correlation between T and SST. We then tested a range of λ to find the maximum correlation. The results are shown in Fig. 2 (solid curves). For the low pass case, this shows the correlation between SST_{lo} and T_{lo} as a function of λ, where T_{lo} is derived from finite

integration of (4) using $Q=Q_{lo}$ and an initial value $T_{lo}=0$. It is clear the optimal values are restricted to a narrow range on the order of 10^{-1} d^{-1} with the peak correlation of 0.85 found at $\lambda=.125$ d^{-1}.

The depth scale h was determined by fitting $SST_{lo}=aT_{lo}+b$ by linear regression to obtain an amplitude ratio $a=6.3\times10^{-2}$ and bias b=29.3ºC. Denoting h as the depth scale for the observed SST, and recalling that $h_c=1$ m was used in computing T_{lo}, it can be seen that $a=h_c/h$. Thus we find that h=16 m gives the optimum fit between the model hindcast and observed low frequency SST variability. For comparison, the mean mixed layer depth, based on a density difference criterion was 14.8 m over the observation period, and the mean Monin-Obukhov scale was 17.4 m (Anderson et al., 1996). Anderson et al. also demonstrated that the layer was often salt-stratified with isohaline layers such as reported by Lukas and Lindstrom (1991). At other times, particularly during day time heating, the layer was thermally stratified. The relatively shallow mean mixed layer depth is accounted for by the buoyancy flux from net precipitation minus evaporation. They showed that the surface freshwater buoyancy flux rate set a critical depth scale of ~16 m such that the net heat loss from solar radiation penetrating the base of the mixed layer equalled the net heat gain at the surface. Based on these and our result, it appears ~16 m is the appropriate mixed layer depth scale for intraseasonal SST variations in the COARE IFA.

The dark curve in the second panel of Fig. 1 illustrates the model hindcast using the full spectrum of the forcing. This was derived from (4) using $Q=Q_{net}$ unfiltered, $\lambda=.125$ and h=16 m as obtained above, and then adding the bias b=29.3ºC to the result. The low frequency variations are well represented whereas the diurnal amplitude and modulation were not reproduced. (Accordingly, the correlation between these curves is not as high as between T_{lo} and SST_{lo}.) The failure to reproduce the diurnal as well as intraseasonal variability with a single set of parameters motivated the separate treatment of these bands. In the following section, we derive a time varying h(t) based on the diurnal amplitude modulation. This was applied to (4) in place of constant h to test whether the low pass hindcast could be improved with a proxy for a variable layer depth. A time varying h(t) will influence the rate of heating

and cooling differently than a constant h. The dashed curve in Fig. 2 shows correlations were slightly degraded at lower frequencies and slightly improved at higher frequencies, while the peak correlation was not significantly affected. Similar results (not shown) were obtained using the observed mixed layer depth variations. A constant layer depth was equally or better suited to hindcast the low frequencies. This indicates that on the intraseasonal time scales SST variations are quite insensitive to shorter term layer depth variations.

Fig. 3 illustrates the model sensitivity to λ, and to a possible bias in the time average Q_{net} during the COARE IOP. Curves in the top panel were computed as above except for setting λ to either 0 or 1 d^{-1}. The latter is about an order of magnitude greater than .125 d^{-1} and the low frequency response is clearly over damped. For λ=0, there is no damping, T becomes the simple time integral of Q_{net} and the lowest frequencies and secular trends are enhanced. The dissimilarity of this evolution to the IMET SST data indicates that the flux variations, such as the increased evaporative cooling during wind bursts, alone did not account for the SST variations on the order of 10−50 days. The trend is due to the mean flux of $\langle Q_{net}\rangle \approx 14$ Wm^{-2} in the IMET observations, where < > denotes time average over the IOP. The bottom panel shows the effect of setting $\langle Q_{net}\rangle=0$ by removing the observed mean while again applying λ=0. The companion curve is the same as Fig. 1. The λ=0; $\langle Q_{net}\rangle=0$ curve has no net trend, but certain trends during late December and the month of February clearly disagree with the observed SST evolution (Fig. 1). We obtained a peak correlation of 0.6 (not shown) by trying various biases with λ=0. This remains significantly smaller than the peak correlation obtained with λ=0.125 (Fig. 2). It is clear that the additional feedback parameterization is necessary and SST cannot be computed with the same fidelity using the surface forcing alone, even if possible measurement biases are considered. With λ>0, the effect of a small $\langle Q_{net}\rangle$ bias is to shift the model to a slightly different equilibrium temperature relative to the initial T. This is illustrated in Fig. A1, where the effect of $r\neq 0$ is to effectively introduce a mean bias in terms of the insolation fraction that penetrates the mixed layer. This bias did not significantly alter the model evolution after the initial λ^{-1} adjustment time. Therefore, the model is insensitive to relatively minor calibration biases in the Q_{net} measurements.

4. Diurnal variability and depth scale

In a like manner to the low pass analysis, we hindcast T_{hi} using $Q=Q_{hi}$ and $h=h_c=1$ m for various values of λ to determine the optimum for the diurnal variations. The feedback model also parameterizes processes regulating SST in the high pass band and demonstrates that the SST diurnal cycle was not a simple time integral of the high pass heat flux. The solid curve marked "high pass" in Fig. 2 shows that $\lambda \approx 5$ d^{-1} is optimum.

With a regression $SST_{hi}=aT_{hi}+b$, we find $h=h_c/a \approx 4$ m for a constant depth scale associated with the daytime heating cycle. The top two panels of Fig. 4 show SST_{hi} and T_{hi}, and it is clear that this hindcast T_{hi} did not simulate the highly variable amplitude. The assumption h=constant was judged inadequate. To estimate a variable h(t), complex amplitude demodulations of SST_{hi} and T_{hi} were computed for both the 1.0 and 2.0 cpd harmonics, using 72 and 36 hour Hanning windows respectively. We denote $amp(SST_{hi})$ and $amp(T_{hi})$ as the root mean square of the diurnal and semi-diurnal amplitudes of the respective signals. Assuming $amp(SST_{hi}) \propto 1/h(t)$ while $amp(T_{hi}) \propto 1/h_c$, we define

$$h(t)=h_c \; amp(T_{hi})/amp(SST_{hi}).$$

As shown in the third panel, Fig. 4, (dark curve) this was generally quite shallow except during episodes of acute deepening. The minimum = 1.2 m, the median = 5.5 m, about 10% exceeded 15 m and the maxima were 20-30 m. Also shown is the mixed layer depth (mld) from Anderson et al (1996) which resolves the diurnal variations. This sometimes extends to >40 m during night-time cooling and strong wind events, and shoals to ~1 m during day-time heating, consistent with the shallow stratified diurnal layers reported by Soloviev and Lukas (1996). The present analysis yields a low pass filtered version due to the complex demodulation being applied over a few cycles, and agrees more consistently with the daily minimum observed mld rather than with the daily average. This is indicative of the shallow thermally stratified layers which form during strong day-time insolation and calm wind

conditions, and lead to large amplitude diurnal SST variations.

The sub diurnal mld variability is influenced by wind-driven mixing, which will act to obliterate shallow stratification and deepen the mixed layer (Anderson et al, 1996). Fig. 4 includes the scalar wind speed measured by the IMET anemometer, filtered with the same 72-hour Hanning window used in the demodulation above. There is a clear coincidence between mld deepening and the wind events (correlation=0.75). The re-computation of T_{hi} using h=h(t) is shown on the bottom panel of Fig. 4. The amplitude modulations now bear a close resemblance to SST_{hi} in the top panel, and the correlation with SST_{hi} is markedly improved as shown in Fig. 2. We found that computing T_{hi} with the diurnally varying observed mld yielded a peak correlation of .82, an improvement over the constant h, but the correlation was not as high as with our h(t) because of the way h(t) was optimized to SST_{hi} amplitudes.

5. Spectral Analyses

A key consideration with the model is the frequency separation between the forcing and response; the ocean acts as a low pass filter and the low frequency components of the forcing dominate the response (Frankignoul and Hasselmann, 1977). The high frequency limit ($f \gg \lambda/2\pi$) is a balance between the first two terms in (1), damping is weak and T resembles a random walk with an f^{-2} spectrum when F is white noise. At low frequencies ($f \ll \lambda/2\pi$) the left hand side of (1) vanishes, damping dominates and T approaches an in-phase response to the low frequency F variations. The transition range of $f \sim \lambda/2\pi$ defines the time scale at which the damping processes parameterized by $-\lambda T$ become important, that is, the first and last terms of (1) are similar amplitude.

The SST spectra from the IMET data (133 days of hourly samples) and the somewhat longer record from the nearby 2°S 156°E TAO Atlas buoy (McPhaden, 1995; 433 days starting 19 September 1992, daily averages) are shown in Fig. 5. The Q_{net} spectrum is shown for f<2 cpd. Variance is relatively high in the intraseasonal band, near $\lambda/2\pi$, and the spectrum is not

ideally white. This intraseasonal Q_{net} variability is amplified in the SST output of the model (Fig. 1). Nevertheless, Q_{net} is considerably closer to a white spectrum than SST [1]. Superimposed on these are the idealized feedback model spectra $P \sim 1/[f^2 + (\lambda/2\pi)^2]$ (smooth curves) using λ=0.125 d^{-1} (low pass analysis) and λ=5 d^{-1} (high pass analysis). These curves indicate that the spectrum has two overlapping regimes. At the high frequency end, the spectrum undergoes a transition from f^{-2} toward flat where $2\pi f \sim 5$ d^{-1}, or f~0.8 cpd, which is close to the diurnal period. At frequencies f<~2 cpd, the SST spectrum becomes f^{-2} again, suggesting that SST is responding as a simple accumulation of random forcing in this band with minimal damping or feedback. Our low pass λ estimate indicates that another transition occurs near $2\pi f \sim 0.125$ d^{-1}, which corresponds to periods ~50 d. The noise and limited low frequency extent of these spectra make this less distinct, and prevent a reliable estimate of λ with a spectral model fit as in Frankignoul (1985). However, our λ determination is robust (Fig. 2) and the associated theoretical spectrum is consistent with the observed. The transition falls within the frequency band of the intraseasonal Madden-Julian oscillation, or MJO (Madden and Julian, 1971). The implication of these time scales with respect to the mixed layer processes is discussed in section 6.

It can be shown that the phase angle between F and T in Eq. (1) is given by $\tan\theta = 2\pi f/\lambda$. At low frequencies, $\theta \rightarrow 0$ as $f \rightarrow 0$ and the theoretical response has T in-phase with F, whereas at high frequencies $2\pi f >> \lambda$ they are in quadrature. The phase angle is $\approx 45^o$ in the subrange $2\pi f \approx \lambda$. The observed phase spectrum between Q_{net} and SST is shown in Fig. 6. There is a clear trend from $\theta = 90^o$ at the highest frequencies toward $\theta = 0$ at about f=0.3 cpd which crosses $\theta = 45^o$ near $2\pi f \approx \lambda$ for λ=5 d^{-1}. The phase then increases and stabilizes around 45° at f<0.1 cpd. Idealized spectra for the two values of λ are superimposed (heavy lines). The observed phase for lower frequencies appears to be held at about 45° in the band where it

---

[1] The higher frequency portion (f>1 cpd) of Q_{net} has a spectral slope of between f^{-1} and f^{-2} and is not shown. It would be misleading to attribute the f^{-2} slope of the SST spectrum at f>1 cpd solely to stochastic forcing, which would require a white Q_{net} spectrum in that range. Nevertheless, the processes governing the spectra in that band are not of interest here.

would be in quadrature relative to the low pass time scale feedback and in phase at the high pass time scale. This may be a consequence of the overlapping regimes suggested by the power spectra. The phase trend at $2\pi f << 0.125$ remains unresolved because of the limited length of these time series.

6. Discussion:

Upper Ocean Feedback: We consider the mixed layer processes which may account for the SST dissipation or negative feedback implicit in these results. (See also Frankignoul, 1985.) It can be seen from (3) that an anomaly T represents the equivalent heat flux of $\lambda\rho C_p hT$, so that the feedback is $\lambda\rho C_p h$ in units of $Wm^{-2}\,{}^oC^{-1}$. In the high pass band, this yields a very large $1.3x10^3$ $Wm^{-2}\,{}^oC^{-1}$, which pertains only to the diurnal SST variations under the influence of large diurnal solar forcing and nocturnal cooling. With the high pass SST standard deviation of 0.23 ^oC, a nominal feedback flux is ~300 Wm^{-2}, which is of similar amplitude to the Q_{hi} standard deviation of ~270 Wm^{-2}. The required diurnal feedback is therefore of similar magnitude to the diurnal forcing. It may be explained by entrainment mixing and the complex process of diurnal stratification, and nocturnal convection coupled with mixed layer deepening (Richards, et al., 1995; Anderson et al, 1996). Entrainment heating or cooling is given by $w_e\Delta T/h$, where ΔT is the temperature change across the base of surface stratified layer and w_e is the vertical entrainment velocity. This will behave in a feedback manner where symbolically $w_e\Delta T/h \propto \lambda T$. The implied scaling for entrainment velocity is $w_e \sim \lambda h$, or 25-30 md^{-1} for λ=5 d^{-1} and a median h(t) of ~5.5 m. The large mld variations over the daily cycle, which range from a few meters during peak insolation to several tens of meters at night, imply parametric entrainment velocities of this magnitude.

On the longer time scale, we estimate the feedback $\lambda\rho C_p h \approx 95$ $Wm^{-2}\,{}^oC^{-1}$ based on λ=.125 d^{-1} and h=16 m. The influence of diurnal mixed layer variations appears to be integrated over longer periods and we have shown that a constant depth scale, close to the mean mld, is suitable for simulating intraseasonal SST variations. Mixed layer feedback processes may

again be attributed to entrainment, and can provide a warming tendency for cool SST anomalies as well as the reverse. As SST increases, feedback can be attributed to entrainment cooling across the base of the mixed layer. Both nocturnal convection and penetrating solar radiation supply heat that is sequestered below the ~16 m depth level during the subsidence phase of the MJO when winds are light, skies are clear and the daily minimum mld becomes shallow. During wind bursts and the MJO convection phase, surface cooling and mechanical mixing erode the shallow layer. The heat that has been sequestered immediately below becomes available to damp further surface cooling through entrainment warming. An episode of such entrainment warming was observed in the early phase of the westerly wind event beginning on 20 December 1992 by Smyth et al. (1996).

The scaling for the low frequencies implies $w_e \sim \lambda h \approx 2$ md^{-1}. Richards, et al (1995), using data from a 4 day warm pool survey, estimated vertical velocity from a heat budget residual to be 11.6±1.6 md^{-1} for a layer depth of 50 m. Interpolating this to 15 m mld assuming w=0 at the surface gives an estimate of ~3.5 md^{-1} for comparison to our scale of 2 md^{-1}. Sprintall and McPhaden (1994) estimated vertical velocities on the order of 0.5 md^{-1} at 0°, 165° E. Wijesekera and Gregg (1996) report that downward and upward turbulent fluxes varied from 0-40 and 0-20 Wm^{-2} respectively during a 20 day cruise at the start of the COARE IOP. During this episode, our model SST anomalies vary from 0 to 0.5 ^{o}C amplitude (low pass), indicating feedback amplitudes between 0 and ~45 Wm^{-2}, which compare favorably. Smyth et al (1996) observed turbulent fluxes exceeding 100-200 Wm^{-2} during brief episodes in December 1992.

Solar radiation may also be important in the feedback context. The shallow daytime layers permit a significant fraction to penetrate, and this represents a heat loss through the mixed layer base that is coincident with positive SST anomalies. This may appear as a feedback effect, and would certainly account for the required diurnal magnitudes of several hundred Wm^{-2}. To test this, we have included the solar penetration term (Eq. 2) in various feedback model trials, with and without the diurnal mld variability, and found no significant improvement in correlation with observed SST in either the high pass or low pass analyses

when compared with the cases where penetration is ignored and all other factors are unchanged. The solar penetration term affects the forcing amplitude but not the time scale according to the model. On the other hand, Anderson et al. (1996) showed that a mean characteristic depth scale of ~16 m is critical for balancing the mean penetrating solar flux with the mean net surface flux. We also noted above that solar radiation absorbed below a shallow mixed layer can be recovered during mixed layer deepening events, so is not permanently lost. Therefore, the role of solar penetration as a feedback effect is a complicated process that remains unclear.

Lateral advection can regulate SST on a range of time scales, including advection by the mean flow. This implies that λ is on the order of U/L, where U and L are velocity and SST gradient length scales respectively. Anderson, et al. (1996) investigated the mixed layer response with a 1-D dynamic instability model (Price, et al. 1986) and these IMET data and hindcast SST with comparable skill to the results here. However, they were not able to replicate the rapid decrease in SST during the westerly wind burst which in part they attributed to advection. Over the whole experiment, the one-dimensional heat budget was closed to within 5-10 Wm-2, or within the uncertainty of the flux observations, so that on the longer term, vertical processes appear to have dominated over lateral advection during these observations. Cronin and McPhaden (1997) documented the SST variation due to advection at 0, 156E (about 200 km north of the IMET) which was predominant during a major westerly wind burst in October 1992 and negligible at other times. Advection, therefore, appears to have been important to the mixed layer heat budget during certain events, while the long term effect remains unresolved.

Forcing and dissipation time scales: We noted above that the natural dissipation time scale appears to coincide with the quasi-periodic forcing frequency in the diurnal and MJO bands. The coincidence appears quite obvious leads to the conjecture that there may be a dynamic connection such that the characteristic forcing frequency influences the dissipation time scale of the mixed layer dynamics. We propose a possible argument for this which can be examined more rigorously in future studies.

It can be seen that $\lambda \sim \omega$ is that with which the model produces a λT of the same amplitude as dT/dt at frequency ω. When Q has a characteristic quasi-periodic frequency ω, then λT and dT/dt are of equal magnitudes at that frequency in balancing Q in Eq. (3). M in Eq. (2) represents the aggregate mixed layer heat dissipation physics such as vertical mixing, lateral advection, penetrating solar radiation, etc. Observation and modeling evidence clearly indicates that M varies with the surface forcing; the mixed layer dynamics are modified by mechanical mixing and buoyancy flux associated with the diurnal heating/cooling and intraseasonal convective systems that modulate the surface heat flux, so M varies with the same characteristic frequency as Q. We can define the dissipation time scale λ as the ratio of the amplitudes of M and T such that λT is the same magnitude as M. Implicitly then, M must have the same amplitude as dT/dt at frequency ω. We find characteristic time scales which suggest that this order of balance exists at two important forcing frequencies, the diurnal and on the order of the MJO ~50 day period, as noted above.

The model amplitude of T, per unit forcing at a given frequency ω, is $(\lambda^2 + \omega^2)^{-1/2}$, which varies inversely with λ. A large damping implies λ or M are large and the SST response will be weak, and vice versa. The dissipation physics in one way or another depend on the amplitude of the SST anomaly. Assume that there is non-linearity such that the natural dissipation time scale varies parametrically with amplitude scale of SST variability [i.e. its standard deviation]. Then a larger SST amplitude scale would generate a larger dissipation scale and vice versa. However, through the model, larger dissipation forces smaller SST amplitude which, with the assumed parameterization, generates a smaller dissipation scale, which allows larger SST amplitude, and so forth. A stability could be reached where the SST amplitude and dissipation scales are balanced. This, in turn, governs the relative amplitudes of M (ersatz λT) and dT/dt, which we have shown above are alike when $\lambda \sim \omega$. Our empirical determinations of λ suggest that something like this is indeed taking place in nature. Note that an inverse relation between dissipation and SST amplitude would be unstable and not lead to an equilibrium time scale.

7. Summary and conclusions

This study has shown that a parameterization of upper ocean mixed layer processes as a temperature feedback leads to realistic simulations of the SST response to surface heat flux observed during TOGA COARE. This underscores the importance of the thermodynamically active oceanic surface mixed layer to the warm pool heat budget. According to various estimates, the warm pool absorbs a small net downward climatological flux of ~10 Wm^{-2} (Waliser, 1996). This represents a temperature tendency of ~5 $^{o}C\ y^{-1}$ in a 15 m deep surface mixed layer. Clearly, the ocean must export this heat either vertically from the thermodynamically active mixed layer or horizontally from the local heating source region in order to maintain a stable mean SST. It is therefore logical to assume that the associated mixed layer processes will have a regulatory role for SST. Our results suggest that this process is episodic rather than steady, as the mixed layer itself undergoes considerable variations in response to surface forcing (Anderson et al., 1996). As a consequence, we should expect the associated SST regulating processes to be apparent on the prominent time scales of the atmosphere-ocean interactions. A linkage is indicated between the time scales of the forcing and the feedback. This appears to be related to the coupling of mixed layer evolution and SST during the diurnal cycling and intraseasonal variations. We have suggested that a dissipation time scale parameterization dependent on SST amplitude might yield such a linkage between the dissipation time scale and the characteristic forcing frequency.

The magnitude of the apparent feedback is substantial in comparison to other feedbacks associated with air-sea fluxes. The parameters λ=.125 d^{-1} and h=16 m signify an equivalent temperature regulating feedback of $\lambda\rho C_p h \approx 95\ Wm^{-2}\ {}^{o}C^{-1}$. Radiative cloud forcing is estimated to be ~22 $Wm^{-2}\ {}^{o}C^{-1}$ (Ramanathan and Collins, 1991). Latent heat flux feedback of ~7-8 $Wm^{-2}\ {}^{o}C^{-1}$ was estimated by Hartmann and Michaelson (1993). The role of ocean physics is entering the debate regarding recent SST regulation and feedback hypotheses. Clement, et al (1996) discovered a basin wide tropical ocean dynamical thermostat with a feedback of about 20 $Wm^{-2}\ {}^{o}C^{-1}$ using the Zebiak and Cane (1987) model. This was manifested by variations in trade winds and upwelling as the model adjusted to a uniform heat flux anomaly, and was verified with further numerical studies by Seager and Murtugudde

(1997). Waliser (1996) points to the role of larger scale or remotely forced atmospheric variability in limiting the growth of SST, and to the potential role of the state of the upper ocean and response to westerly wind bursts. The apparent upper ocean feedback that we find on intraseasonal and shorter time scales leads to a significantly reduced SST sensitivity to variations in the net heat flux. Gent (1991) estimated an SST sensitivity in the warm pool of 0.1 $^{o}Cm^{2}W^{-1}$, which is the inverse of a feedback of ~10 Wm^{-2} $^{o}C^{-1}$. Our results indicate that SST is about an order of magnitude less sensitive (~0.01 $^{o}Cm^{2}W^{-1}$) to a flux anomaly than Gent's result, which was obtained from model simulations forced with monthly mean climatological winds so that the MJO variability was not represented. Given that our results indicate important influences regulating SST occur in this band, climate models that rely on monthly mean fields may be significantly limited in this respect unless a parameterization for this SST regulation is included. We should note that our larger time scale λ^{-1}=8 days remains about an order of magnitude smaller (therefore larger feedback) than the 2-6 month time scales found in the mid-latitude Pacific by Frankignoul and Reynolds (1983). Indeed, the duration of our 4-month time series is on that order and such time scales may not be resolvable in our analysis, although Fig. 2 indicates that our result is quite robust and time scales of a month or longer would yield relatively poor correlation. Frankignoul and Reynolds analyzed monthly SST anomalies which, in turn, do not have the temporal resolution to detect such short time scales as we find. Nevertheless, the disparity between these scales might best be ascribed to differences between the tropical warm pool and mid-latitude air-sea interaction processes.

The appropriate depth scale for the thermodynamically active mixed layer was found to be 16 m for these observations, which compares favorably with the mean mld, the Monin-Obukhov scale and compensation depth described by Anderson et al, 1996. Coupled models such as Zebiak and Cane (1987) use a 50 m mld, which is evidently too deep for the warm pool. The shallower scale is governed by the rate of freshwater buoyancy flux (Anderson et al, 1996; Shinoda and Lukas, 1995) and tends to isolate the water between this level and the top of the thermocline from direct contact with the atmosphere. However, the observed mld varied considerably over tens of meters during night-time convection and during wind events, so

some heat exchange must occur with the adjacent layers below the 15-16 m depth scale. Night-time convection sequesters some heat below the shallow day-time heating layer, which can be partially recovered when the mixed layer deepens during the MJO cooling events. Likewise, the shortwave radiation which penetrates the shallow mixed layer is mostly absorbed in the upper 30 m and can be retrieved both during the night-time convection and during the strong wind events. These processes may tend to impart a time averaging effect over the varying mld. The diurnal SST range is controlled by the daily minimum mld, which is in turn controlled by the MJO wind forcing. The differential between diurnal heating and nocturnal cooling determines the SST tendency over the MJO cycle. Therefore, there are important mixed layer processes which interact across the diurnal to MJO time scales, which control SST and the depth scale.

Lastly, Anderson et al (1996) investigated the mixed layer response with a 1-D dynamic instability model (Price, et al, 1986) and these IMET data and hindcast SST with comparable skill to the results here. Further resolving the positive and negative feedbacks in the western Pacific warm pool will require careful numerical experimentation with fully coupled ocean-atmosphere models which accurately describe the physics of the boundary layers on both sides of the air-sea interface, as well as atmospheric deep convection, and which are capable of treating the multiple time- and space-scale interactions which appear to be crucial. The feedback model results here emphasize that the diurnal and intraseasonal time scale ocean mixed layer processes need to be properly treated, as they may be fundamentally important in regulating the warm pool SST.

Acknowledgements: This work was supported under NASA contract NASW-4824, NASA grant NAS5-31722 and NSF grants OCE96-23168, OCE91-10599 and OCE91-13948. TOGA TAO SST data were furnished by NOAA/PMEL.

Appendix:

The mixed layer transparency was estimated as

$$r = 0.62\exp(h(t)/0.6) + 0.38\exp(h(t)/20) \qquad \text{(A1)}$$

from Paulson and Simpson (1977). Fig. A1 illustrates the low pass result with the transparency coefficient r=0.2 (for h~15 m) vs r=0. The curves do not differ in any significant manner which would affect the stochastic model interpretations given in the text with regard to the scales and processes related to the MJO. The two curves are shown plotted about their respective means, which differed by ~0.4°C because the stochastic model adjusts to the mean Q_{net}-rQ_{sw}, which is lessened when r≠0. The adjustment time is ~1/λ which accounts for the discrepancy between these curves at the start of the record. The highest correlations between model and observed temperature were found for r=0 when this initial transient was not included in the correlation.

For the high pass, r(h) was computed from (A1) using h(t) derived in the Section 3. This resultant hindcast was nearly identical with that shown in Fig 3, except with the amplitude reduced by about 30%. Re-scaling the hindcast amplitude would require decreasing h(t), which in turn adjusts r=r(h) and so on. Use of the observed layer depth degraded the correlation relative to that obtained with our h(t). We conclude that the scale of h(t) shown in Fig. 3 may be biased high by ~30% due to the assumption of r=0, and caution is advised in interpreting the absolute magnitude of h(t) as shown. The nature of the h(t) variations would not be affected, however, nor would the high pass damping scale λ.

References:

Anderson, S.P., R.A. Weller and R. Lukas, 1996: Surface buoyancy forcing and the mixed layer of the Western Pacific warm pool: Observations and 1-D model results, J. Climate, 9, 3056-3085.

Clement, A., R. Seager, M. Cane and S. Zebiak, 1996: An ocean dynamical thermostat. J. Climate, 9, 2190-2196.

Croinin, M.F. and M.J. McPhaden, 1997: The upper ocean heat balance in the western equatorial Pacific warm pool during September-December 1992. J. Geophys. Res., 102, 8533-8553.

Fairall, C.W., E.F. Bradley, D.P. Rogers, J.B. Edson and G.S. Young, 1996: Bulk parameterization of air-sea fluxes for TOGA COARE. J. Geophys. Res., 101, 3747-3764.

Frankignoul, C., 1983: Sea surface temperature anomalies, planetary waves and air-sea feedback in the middle latitudes, Rev. Geophys., 23, 357-390.

Frankignoul, C. and K. Hasselmann, 1977: Stochastic climate models, Part II, Application to sea-surface temperature anomalies and thermocline variability. Tellus, 29, 289-305.

Frankignoul, C., and R.W.Reynolds, 1983: Testing a dynamical model for mid-latitude sea surface temperature anomalies, J. Phys. Oceanogr., 13, 1131-1145.

Gent, P.R., 1991: The heat budget of the TOGA COARE domain in an ocean model. J. Geophys. Res., 96, suppl., 3323-3330.

Hartmann, D.L. and M. Michaelsen, 1993: Large-scale effects on the regulation of tropical sea surface temperature. J. Climate, 6, 2049-2062.

Hasselmann, K., 1976: Stochastic climate models, Part I. Theory, Tellus, 28, 473-484.

Hosum, D.S., R.A. Weller, R.E. Payne and K.E. Prada, 1995: The IMET (Improved Meteorology) ship and buoy system. J. Atm. Oceanic Tech., accepted

Jenkins, G.M. and D.G. Watts, 1968: Spectral analysis and its applications, Holden-Day, San Francisco, 525 pp.

Lagerloef, G.S.E., 1995: Interdecadal variations in the Alaska Gyre, J. Phys. Oceanogr., 25, 2242-2258.

Lukas, R. and E. Lindstrom, 1991: The mixed layer of the western equatorial Pacific Ocean, J. Geophys. Res., 96, suppl., 3343-3357.

Madden, R. and P. Julian, 1971: Detection of a 40-50-day oscillation in the tropical Pacific., J. Atm. Sci., 28, 702-708.

Manabe, S. and R. Stouffer, 1996: Low-frequency variability of surface air temperature in a 1000-year integration of a coupled atmosphere-ocean model., J. Climate, 9, 376-393.

McPhaden, M.J., 1995: The Tropical Atmosphere Ocean Array is completed, Bull. Am. Meteo. Soc.., 76, 739-741.

Paulson, C.A. and J.J. Simpson, 1977: Irradiance measurements in the upper ocean, J. Phys. Oceanogr., 7, 952-956.

Price, J., R. Weller and R. Pinkel, 1986: Diurnal cycling: Observations and models of the upper ocean response to diurnal heating, cooling and wind mixing., J. Geophys. Res., 91, 8411-8427.

Ramanathan, V. and W. Collins, 1991: Thermodynamic regulation of ocean warming by cirrus clouds deduced from observations of the 1987 El Niño., Nature, 351, 27-32.

Richards, K.J., M.E. Inall and N.C. Wells, 1995: The diurnal mixed layer and upper ocean heat budget in the western equatorial Pacific, J. Geophys. Res., 100, 6865-6880.

Shinoda, T. and R. Lukas, 1995: Lagrangian mixed layer modeling of the western equatorial Pacific, J. Geophys. Res., 100, 2523-2541.

Seager, R. and R. Murtugudde, 1997: Ocean dynamics, thermocline adjustment, and regulation of tropical Pacific SST. J. Climate, 10, 521-534.

Siegel, D.A., J.C. Ohlman, L. Washburn, R.R. Bidigare, C.T. Nosse, E. Fields and Y. Zhou, 1995: Solar radiation, phytoplankton pigments and radiant heating of the equatorial Pacific warm pool., J. Geophys. Res., 100, 4885-4891.

Smyth, W.D., D. Hebert and J. Moum, 1996: Local ocean response to a multiphase westerly wind burst, 2. Thermal and freshwater responses. J. Geophys. Res., 101, 22,513-22,534.

Soloviev, A. and R. Lukas, 1996: Large diurnal warming events in the near-surface layer of the western equatorial Pacific warm pool, J. Geophys. Res., submitted.

Sprintall, J. and M. McPhaden, 1994: Surface layer variations observed in multiyear time

series measurements from the western equatorial Pacific., J. Geophys. Res., 99, 963-979.

Waliser, D.E., 1996: Formation and limiting mechanisms for very high sea surface temperature: Linking the dynamics and thermodynamics. J. Climate, 9, 161-188.

Webster, P.J. and R. Lukas, 1992: TOGA COARE: The Coupled Ocean-Atmosphere Response Experiment, Bull. Am. Meteo. Soc.., 73, 1377-1416.

Weller, R.A. and S.P. Anderson, 1996: Surface meteorology and air-sea fluxes in the western equatorial Pacific warm pool during the TOGA Coupled Ocean-Atmosphere Response Experiment. J. Climate, 9, 1959-1990..

Wijesekera, H. and M. Gregg, 1966: Surface layer response to weak winds, westerly bursts, and rain squalls in the western Pacific Warm Pool, J. Geophys. Res., 101, 977-998.

Zebiak, S. and M. Cane, 1987: A model El Niño-Southern Oscillation, Mon. Weather Rev., 115, 2262-2278.

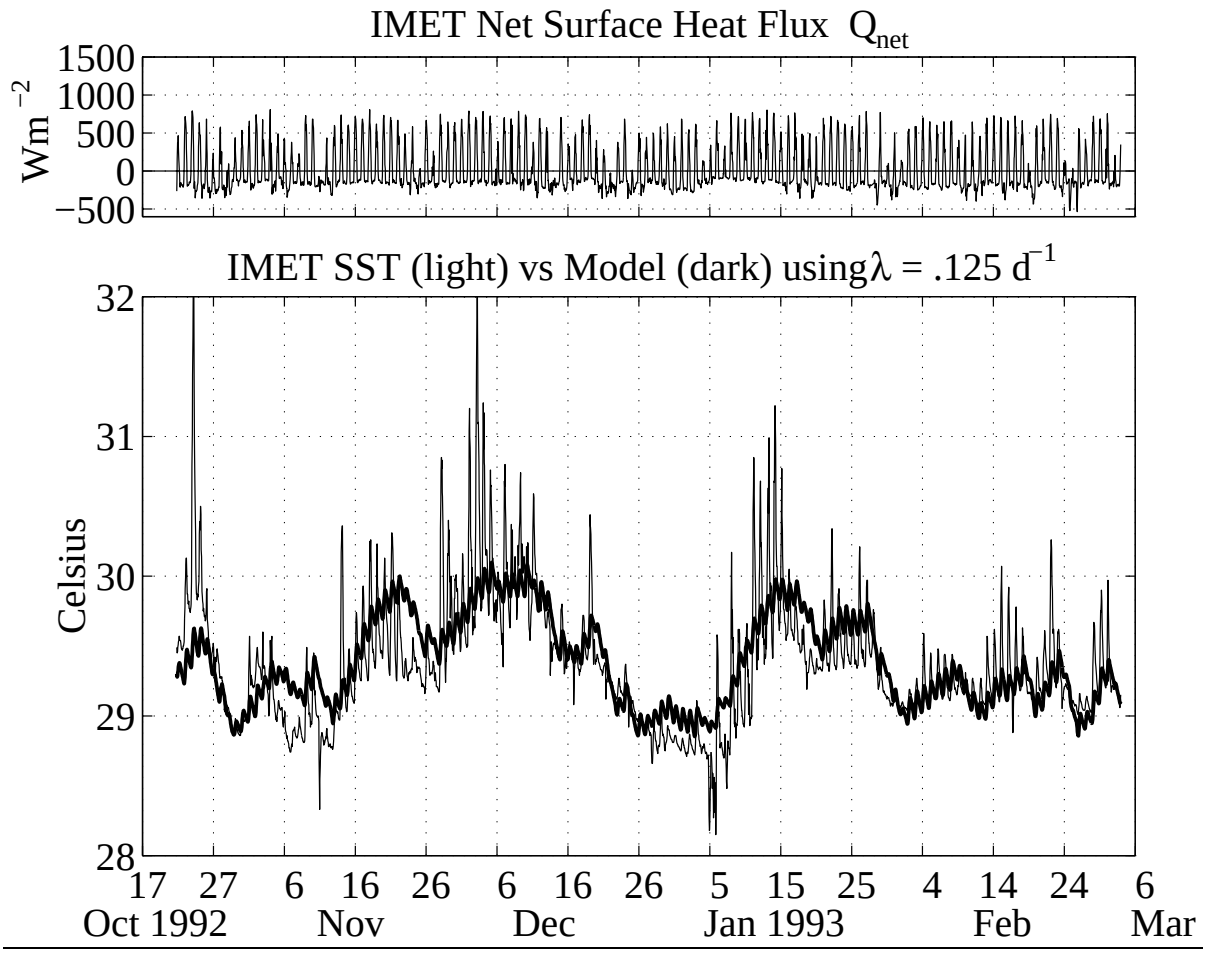

Fig. 1. Top panel: Net surface heat flux measured by the WHOI IMET buoy. Middle panel: observed 0.45 m SST (light curve) and feedback model hindcast (dark curve) with damping coefficient, λ=0.125 d^{-1}, which provides the best correlation between the model and observed SST.

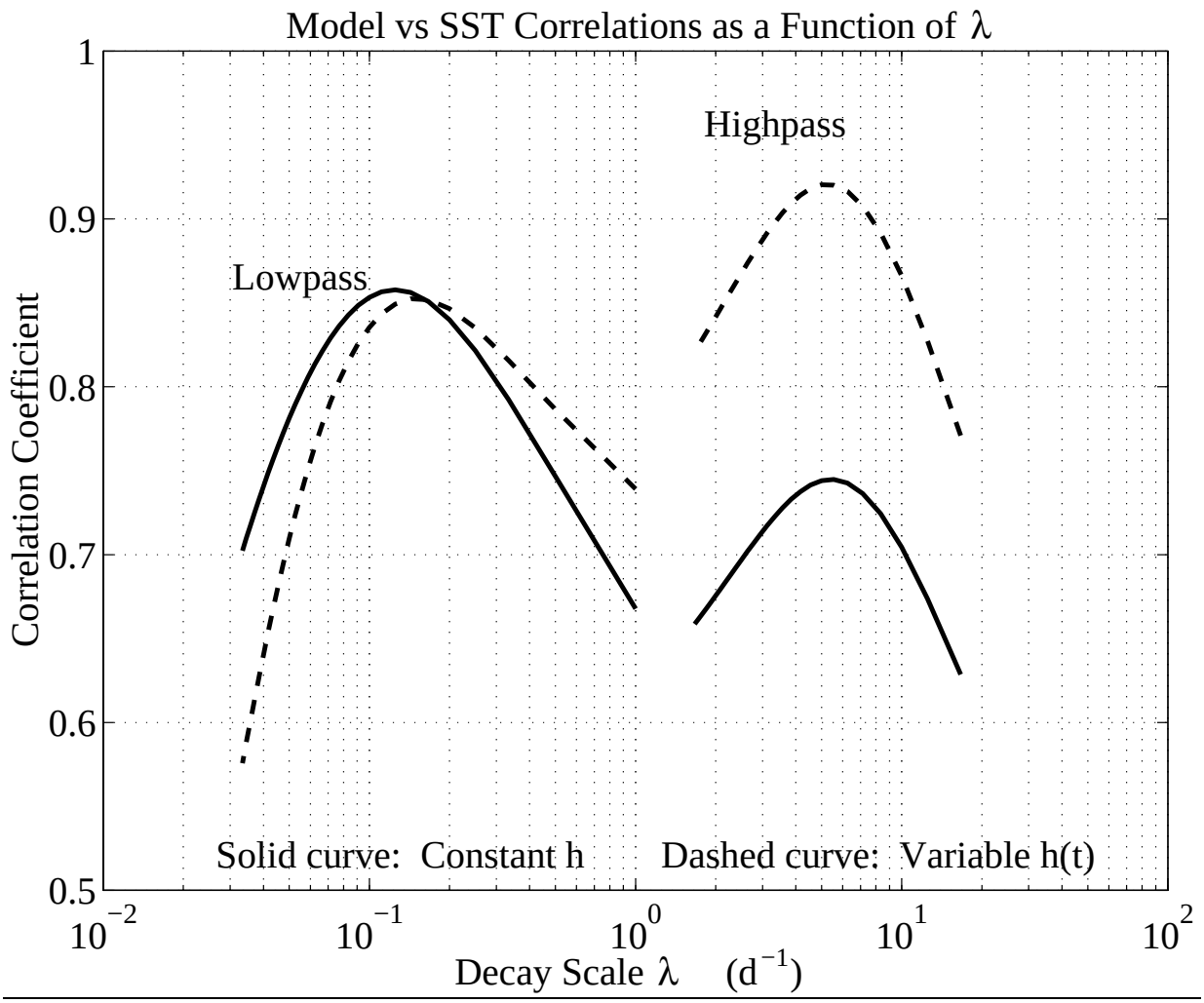

Fig. 2. Correlations between observed SST and stochastic model as a function of coefficient λ for both the low pass and high pass analyses. The optimal λ values were determined from the curve maxima. Solid curves are for a constant depth scale h. Dashed curves are when time varying h(t) was used in the feedback model, where h(t) was determined from diurnal amplitude demodulation as described in the text.

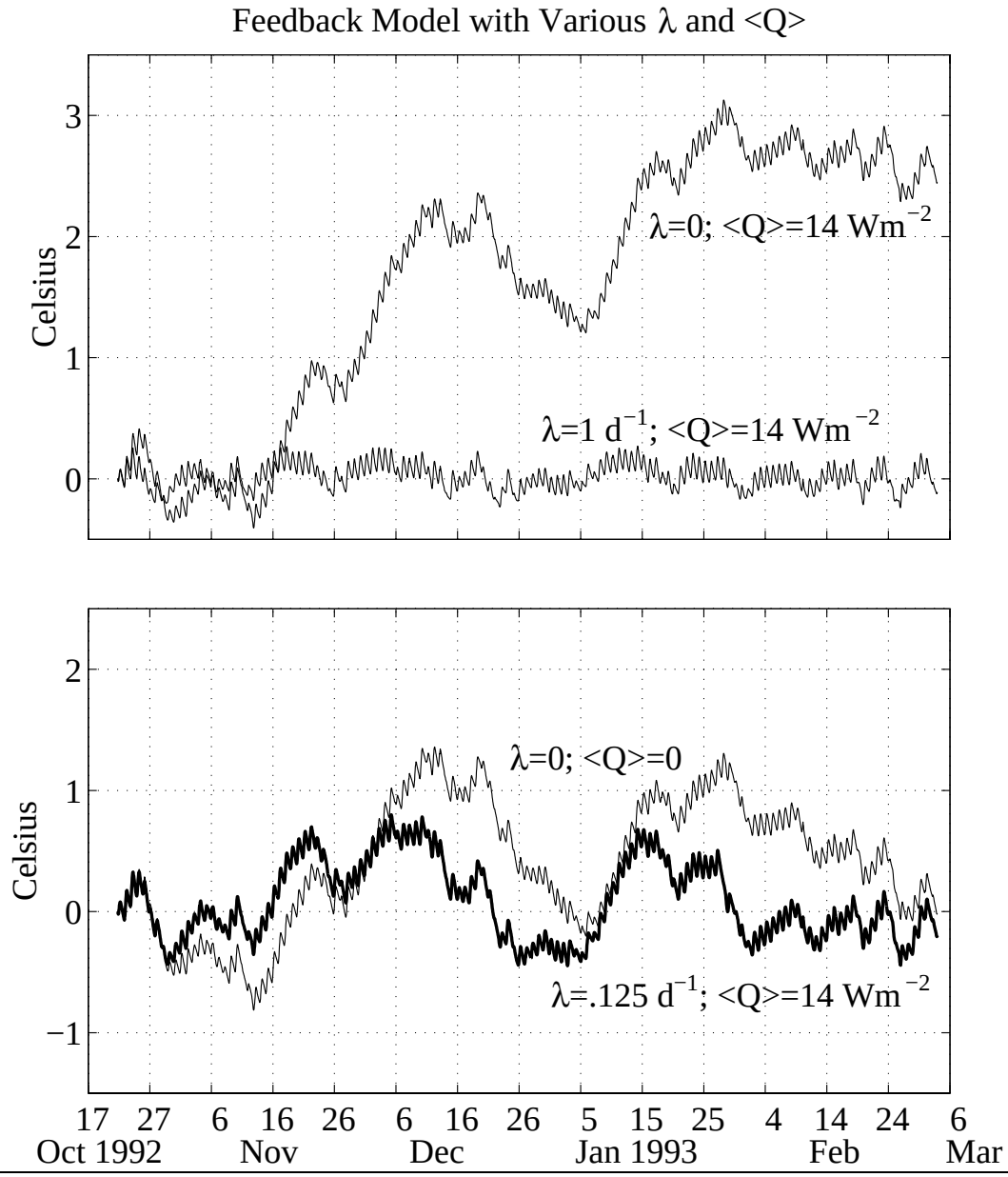

Fig. 3. Top panel: For λ=0 the stochastic model is the simple time integral of Q_{net} and is biased toward low frequencies. For λ=1 d^{-1} the stochastic model is over-damped. Bottom panel: Setting <Q>=0 while keeping λ=0 (light curve) has larger response and phase shift at lower frequencies relative to the simulation with feedback (dark curve; same as Fig. 1), which better represents the observed SST. This indicates that the feedback term represents important physical process is not simply accounting for errors or bias in the forcing term.

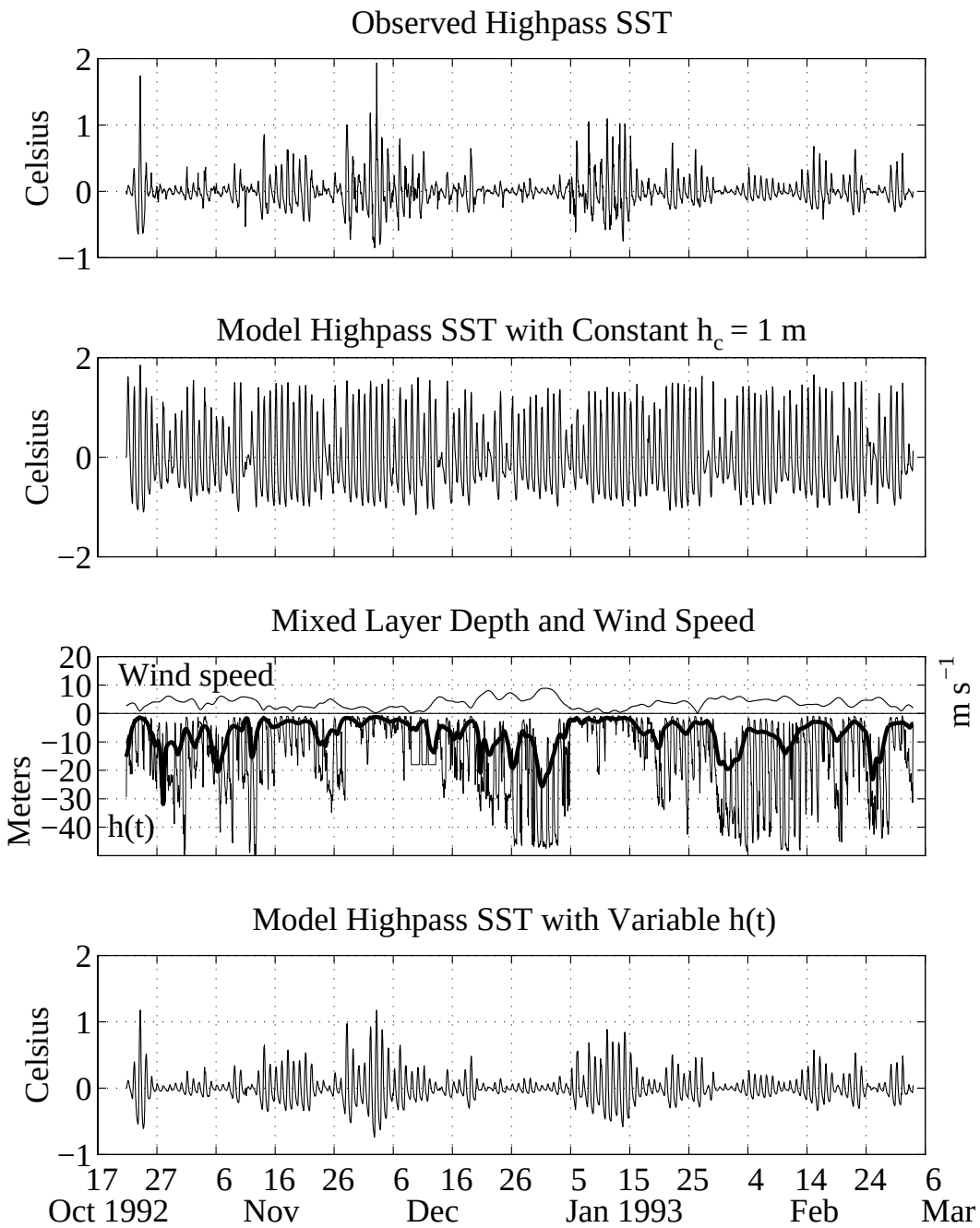

Fig. 4. First panel: High pass temperature showing diurnal amplitude modulations. Second panel: Model hindcast assuming a constant diurnal mixed layer depth of 1 m, which does not reproduce the modulation. Third panel, below abscissa: Estimated (dark) and observed (light) variable mixed layer depth h(t). Above abscissa: Wind speed. Fourth panel: Model hindcast using the estimated variable diurnal mixed layer depth h(t), which yields a much improved simulation of the first panel.

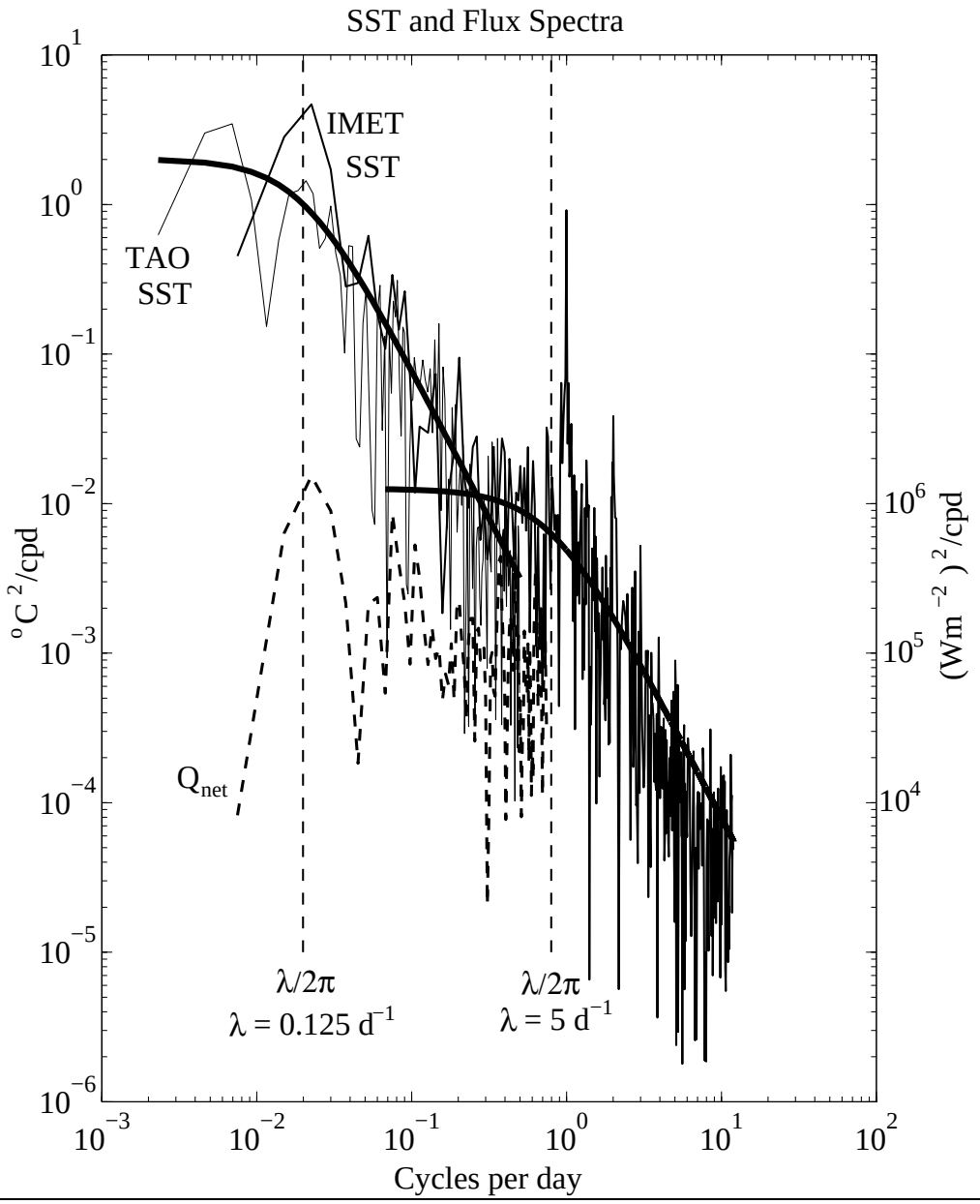

Fig. 5. The SST spectra from IMET (133 days of hourly samples) and the 2ºS 156ºE TAO Atlas (433 days starting 19 Sep 92, daily averages). Superimposed on these are the idealized stochastic model spectra $P \sim 1/[f^2 + (\lambda/2\pi)^2]$ (smooth curves) using λ=0.125 d^{-1} and λ=5 d^{-1}. Two overlapping regimes are evident. At the high frequency end, the spectrum transitions from f^{-2} toward a white spectrum where $f \sim \lambda/2\pi$, or f~0.8 cpd (vertical dashed line). At lower frequencies the spectrum becomes f^{-2} again until $f \sim 0.125/2\pi$, which corresponds to periods ~50 d. The near-white Q_{net} spectrum for f<2 cpd is also shown (dashed curve).

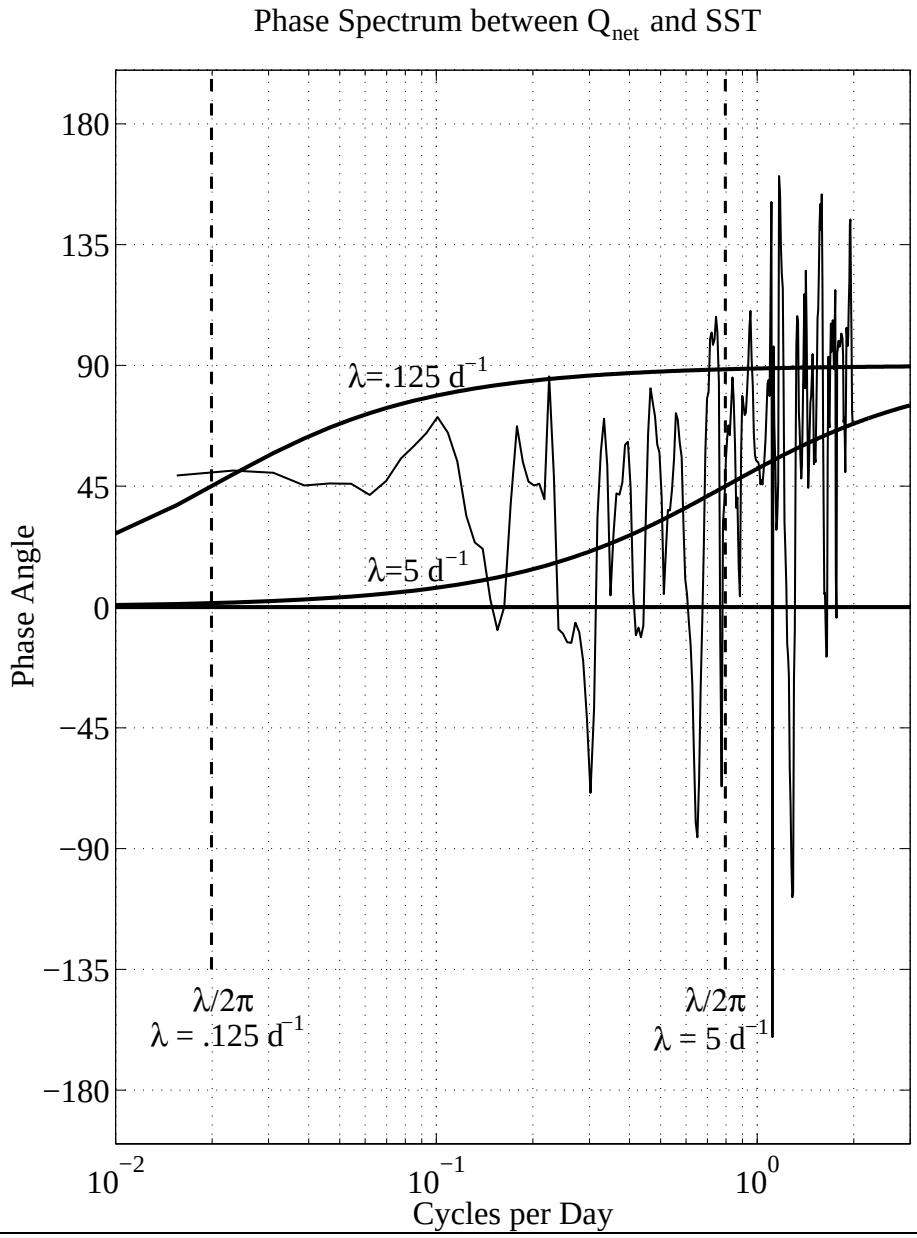

Fig. 6. Light curve: Phase spectrum between Q_{net} and SST measured at the IMET buoy (bin averaging every 5 frequency bands of the co- and quadrature spectra before computing phase). Dark curves: Ideal feedback model phase spectrum, arctan($2\pi f/\lambda$), for λ=0.125 d^{-1} and λ=5 d^{-1} as derived for the low pass and high pass analyses respectively. The phase is ideally 45° when $2\pi f=\lambda$, and appears to be influenced by both diurnal and MJO related processes in the intervening frequency bands.

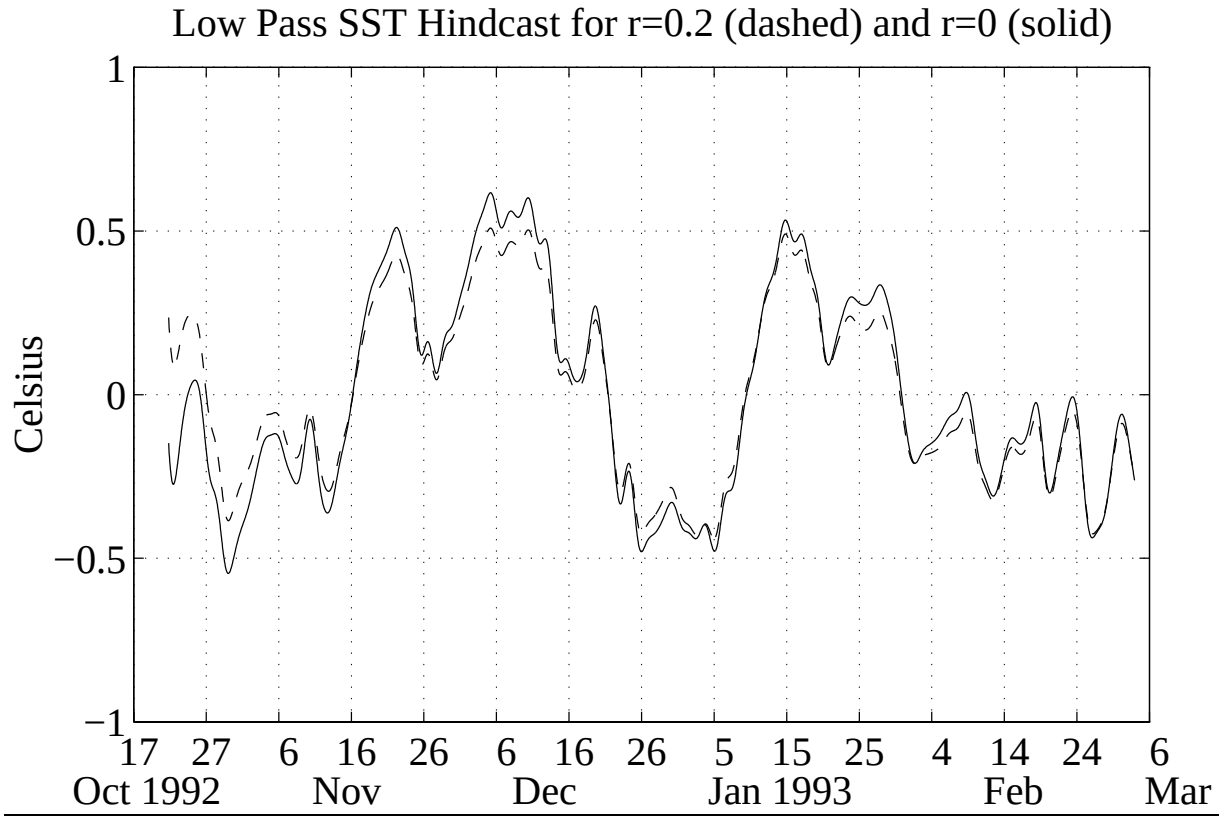

Fig. A1. The low pass hindcast result with the transparency coefficient r=0.2 (dashed curve) vs r=0 (solid curve), plotted relative to their respective mean.